UNIVERSITY OF BIRMINGHAM

Research at Birmingham

Pulsed discharge regeneration of diesel particulate filters

Graupner, K.; Binner, Jon; Fox, N.; Garner, C. P.; Harry, J. E.; Hoare, D.; Ladha, K. S.; Mason, A.; Williams, A. M.

[Link to publication on Research at Birmingham portal](#)

Pulsed discharge regeneration of diesel particulate filters

K Graupner[1], J Binner[2], N Fox[3], C P Garner[1], J E Harry[1], D Hoare[1], K S Ladha[1], A Mason[1] and A M Williams[1]

[1] Wolfson School of Mechanical and Manufacturing Engineering, Loughborough University, Leics LE11 3TU, UK

[2] Aeronautical, Automotive, Chemical and Materials Engineering, Loughborough University, Leics LE11 3TU, UK

[3] 3DX-RAY Limited, 16 & 18 Hayhill Industrial Estate, Sileby Road, Barrow-upon-Soar, Loughborough, LE12 8LD, UK

E-mail: `M.K.Graupner@lboro.ac.uk`, `C.P.Garner@lboro.ac.uk`, `A.M.Williams@lboro.ac.uk`

Abstract. A novel method to effectively remove soot from a diesel particulate filter using pulsed electric discharges is presented. Fast rising high voltage pulses of between 18-25 kV of nano- to microsecond duration with pulse energies of typically 100 -200 mJ are applied to the filter via a spark gap. The initial removal process proceeds via the formation of microdischarges which slowly erode the soot layer. Subsequently spark discharges occur which remove the accumulated soot more effectively from a larger filter volume. Regeneration is complete when the soot cake layer is eliminated. Average soot removal rates of ~ 0.1 - 0.2 g/min were achieved at 50 Hz breakdown frequency by optimizing electrode geometry, breakdown voltage and capacitor size. On-engine long term testing of the technology showed soot removal by pulsed discharge to be reliable, efficient and uniform; a total of 100 g of soot was deposited and removed over 18 filter regeneration cycles.

1. Introduction

The diesel particulate filter (DPF) is an accepted technology for particulate matter removal from engine exhaust gases from modern on and off-road diesel engine applications. A significant proportion of particulate mass produced by diesel engines is in the form of nanoparticles which are suspected of having adverse health effects in humans [1].

DPFs are made from cordierite or silicon carbide and due to their unique structure are capable of filtering emitted soot particles below tens of nanometers in size. A honeycomb structure is commonly used for a wide range of filters and catalysts due to its large exposed surface area. A schematic of the structure and soot trapping mechanism of a honeycomb cordierite DPF is shown in Fig. 1. Particulate matter is trapped in the porous walls of the filter as deep bed soot and as a cake layer on the filter walls. The filtration efficiency of the filter increases with accumulated soot; as the porous walls are filled up, less and less particulates can traverse the filter without being trapped [2].

As the filter fills up with soot, flow resistance increases and a pressure differential establishes over the filter. The steadily increasing engine back pressure creates a significant fuel consumption and engine performance penalty. The particulate filter must be regenerated (cleaned) at regular intervals, typically when a soot load of several grams per litre filter volume is deposited. Conventionally the soot trapped in the filter is incinerated in oxygen rich diesel exhaust gas by means of an electric heater, high-temperature afterburner or at suitable engine operating conditions when the exhaust temperatures are sufficiently high. Temperatures of 500-600°C are usually necessary to start incineration. System melting or cracking of the DPF may occur due to thermal runaway caused for example by an uneven soot distribution within the filter. Soot levels have to be monitored as there is an upper limit for the incineration to avoid excessive temperatures and temperature gradients. Repair or replacement of damaged or overloaded filters is very costly and time consuming. Additives or catalysts can be added to the fuel or filter substrate to enable incineration at lower temperatures, however, filter damage is still possible.
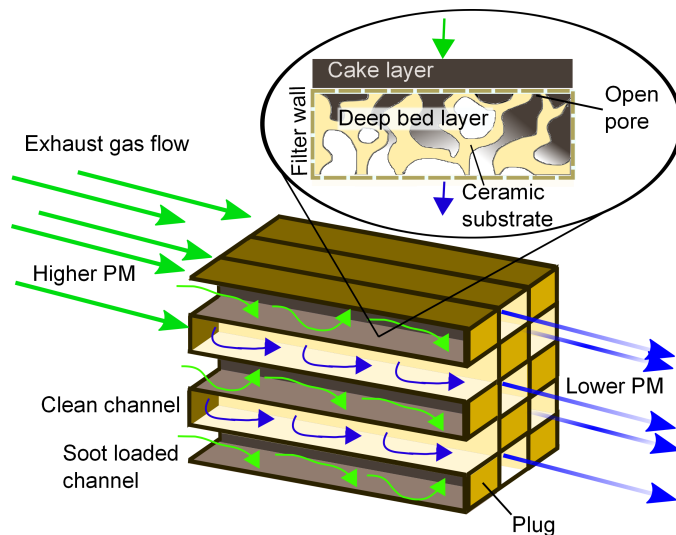
Figure 1: Principle of diesel particulate filter operation: particulate matter from the engine exhaust is collected in the narrow channels of the DPF.

In this paper an entirely new way of regenerating a diesel particulate filter using a pulsed discharge is presented. This work is noteably different to previously published data reporting a different electric discharge technique to remove soot from a DPF by oxidation [3].

Previous research into plasma treatment of diesel particulate filters by other research groups has focused on the creation of active oxygen species or ozone produced for example by barrier discharges which then erode the soot via oxidation reactions. The plasma itself may be produced outside or inside the filter; addition of oxygen [4] or nitric oxide [5] to the exhaust stream accelerates the regeneration. There are, of course, major practical and safety issues associated with adding compressed, potentially harmful gases to on and off-road applications. A different strategy is to remove particles directly from the exhaust stream by use of a plasma reactor [6]. The challenge is to obtain sufficiently high removal rates with low power consumption. Direct plasma treatment of diesel soot deposited on a small electrode has been reported [7]. Here a dielectric surface barrier discharge was employed to remove soot particles under formation of microdischarges. This system has only been shown to work with a single flat electrode. Indeed, it has proved difficult to generate a plasma evenly inside the honeycomb substrate. Creation of stable dielectric barrier discharges in capillaries and honeycombs has been investigated in detail by Hensel et al. [8–10]. Accidental sparking, hot spots and streamers creating holes in cordierite walls thereby compromising the filter integrity and filtration behaviour have previously been identified as problematic [9, 11].
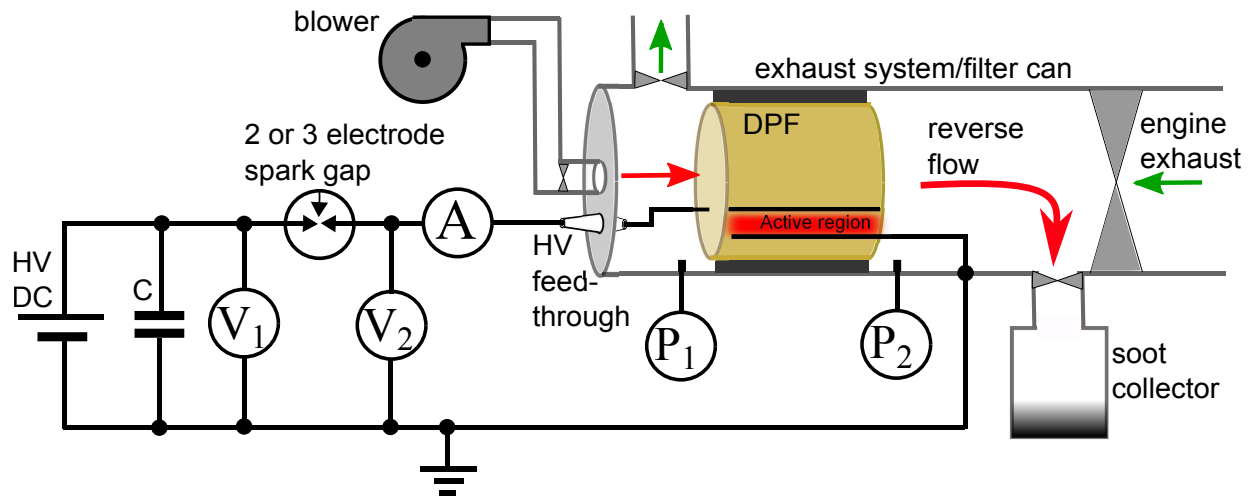
Figure 2: Basic operation principle of the DPF regeneration system. During filter soot loading the differential pressure over the filter is evaluated with static pressure sensors P_1 and P_2. Soot is removed from the active region by discharging a capacitor into the filter via a spark gap. A small reverse flow transports the loose soot to a soot collector adjacent to the filter. The voltage across the capacitor is measured with high voltage probe V_1 and the voltage across the filter with high voltage probe V_2.

2. Experimental apparatus and method

A simplified schematic of the experimental setup is shown in Fig. 2. An energy storage capacitor (700 pF) was discharged via a variable, two electrode or biased, three-electrode spark gap switch [12] at voltages between 15 and 30 kV. A spark gap is still the most economical way to achieve fast voltage risetimes in the order of $\sim 1 \text{kV/ns}$ in conjunction with high transmitted currents >100 A. The high voltage power supplies used in the experiment are based on conventional high voltage technology [12]. The particulate mass regeneration rate (g/min) depends on the frequency of breakdown in the filter, applied initial voltage, soot loading, electrode geometry and system capacitance. Average regeneration rates of $\sim$ 0.1 - 0.2 g/min (per high voltage supply, Fig. 2) were achieved at a breakdown repetition rate of 40 Hz. The regeneration rate can be further increased and tailored to the application, for example by increasing the breakdown repetition rate. Particulars of system integration are not considered in detail in this paper which instead reports for the first time operation principles and focuses on fundamentals of soot removal by the discharge. The voltage was measured at two positions, across the energy storage capacitor (V_1) and the filter (V_2) using a wide-band voltage probe (Tektronix P6015A), Fig. 2. Measurement across the capacitor was generally favoured as a voltage probe connected to the floating part of the spark gap was found to influence breakdown behaviour as it provided a resistive path to ground (100MΩ). A current probe (Pearson current monitor 411) was located between the spark gap and the filter. The probe signals were recorded on a Tektronix TDS 5034B oscilloscope (350 MHz, 5 Gsamples/s).
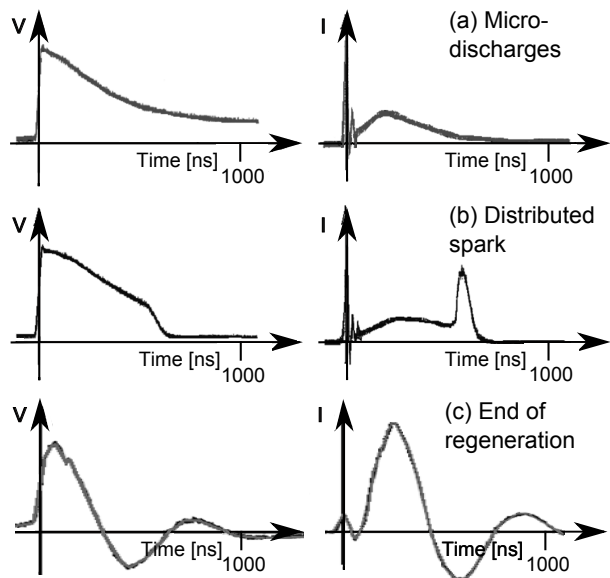
Figure 3: Overview over typical current and voltage waveforms for single pulses observed during regeneration. The regeneration progresses through (a)-(b)-(c). The voltage was measured at position 2, across the filter.

The tests had two stages: loading and regeneration. Filters were soot loaded on a 4 cylinder Tier 2 heavy duty engine. Engine run conditions for loading were held at 1200 rpm/250 Nm. The pressure was measured post- and pre-DPF, the maximum differential pressure (P_1-P_2) for each filter loading was set to 235 mbar to remain within normal engine limits. During regeneration a small reverse air flow of up to 15 l/min removed the regenerated particulate matter from the filter.

The active region serviced by the discharge is shown schematically in Fig. 2 and is located between high voltage and grounded electrodes inserted fully into the filter. The high voltage steel electrodes were inserted on the clean filter side. The grounded electrodes were made of tinned copper wire (22 AWG) and were inserted on the sooty filter side. There are a number of constrains on the possible electrode geometries due to the honeycomb structure; best regeneration results were achieved with grounded rectangular shapes with a row of high voltage electrodes located in the centre. By combining several identically sized, optimized electrode rectangles, the active region was readily extended over the whole filter volume. The filter type used in the experiments was uncoated 5.66 inch × 6 inch (144 mm × 152 mm), 100 cpsi (cells per square inch) cordierite honeycomb.

3. Progression of regeneration

Soot removal from the filter progresses in three different stages. When the fast rising high voltage pulse created by the spark gap is first applied to a freshly soot loaded filter a distributed, resistive current flows for around 500 ns, Fig. 3a. Microdischarges are
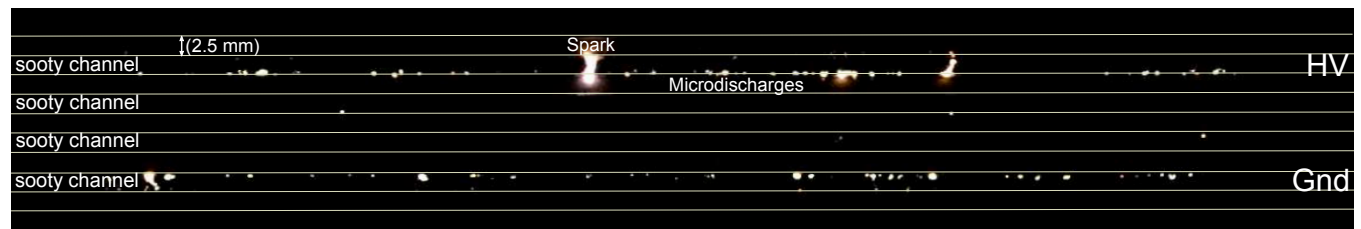
Figure 4: Microdischarges typically occur at the beginning of the regeneration. This image is an overlay of approximately 150 frames recorded at 10 frames/second, showing a birds eye view of a sectioned filter. A single high voltage and grounded electrode were used to drive the discharge and are located one channel below the viewing plane. Microdischarges occur along the whole length of the filter, mainly in the corners of the soot filled channels adjacent to the electrodes and often reoccur in the same location.
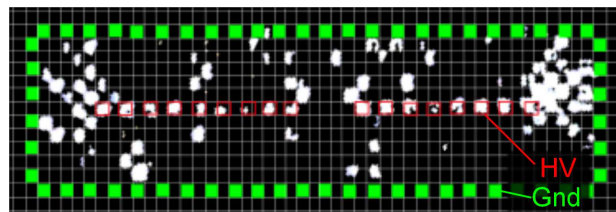

Figure 5: Distribution of spark discharge in the filter volume during regeneration, viewed axially. This image is an overlay of approximately 1300 images taken at 25 frames/second and represents ∼10% of regeneration after the microdischarge stage. The grounded electrodes (green) are assembled in a rectangular shape around a row of interconnected high voltage electrodes (red). Note that only few of all the spark discharges occurring in the filter will be visible as only clean channels can be seen, furthermore not every pulse is capable of forming a spark. The spark is distributed over the volume but there are preferred paths towards the corners of the grounded rectangle.

observed in the sooty channels, mainly adjacent to the electrodes and located in the channel corners, as shown in Fig. 4, weakly eroding the soot layer. Breakdown occurs in air gaps between channels and probably between particle-particle contacts. Soot may be incinerated or loosened by the high temperatures and expanding air occurring around the microdischarges.

During the next stage a spark discharge forms in the filter, Fig. 3b. The spark energy is concentrated in a short pulse of ∼ 300 ns duration. Luminous filamentary spark discharges are observed throughout the active region, Fig. 5. The spark discharge is capable of traversing the highly porous filter walls without observable damage and effectively removes the accumulated particulate matter by shock formation in the surrounding air. Further experiments indicated that the spark discharge preferably forms in locations where soot remains. However, electrode geometry and especially the distance to the nearest grounded electrode influence the spark discharge behaviour more
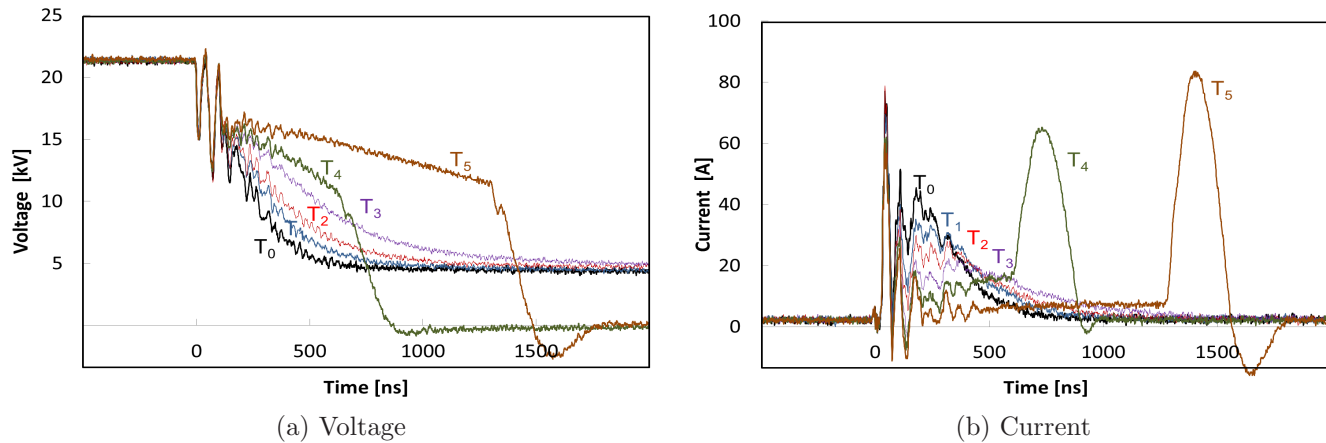
Figure 6: Voltage (a) and current (b) waveforms during progression of the regeneration. Individual discharges follow each other as $T_0 < T_1 < T_2 < T_3 < T_4 < T_5$. Some ringing is observed on both probe signals due to system inductances. Note that the voltage is measured across the capacitor (V_1).

strongly, Fig. 5.

At the end of the regeneration underdamped LC oscillations occur, Fig. 3c. At this stage the spark discharge is usually formed in only spot in the filter. As currents are exchanged for considerable times $>1\mu s$ at certain locations within the filter, localized melting and pinhole damage (diameter $<100\mu m$) to the filter substrate occurs. Only very few pinholes form in the filter volume. Their size is comparable to maximum pore sizes occurring naturally in the substrate of a new filter [13]. No change in filtration efficiency has been observed and is therefore of no concern.

Voltage and current waveforms recorded during the first two stages of regeneration are shown in more detail in Fig. 6a and 6b. Displacement currents from charge redistribution peak immediately after breakdown, originating from charge redistribution during the initial spark gap breakdown and the charging up process of the equivalent capacitance of the wires, filter and electrodes (at most a few tens of pF) in parallel with the energy storage capacitance. The measured displacement currents did not vary with soot loading and the signal is probably partly due to probe overshoot and ringing. The displacement current flow is followed by the resistive current after a short time lag of ~ 100 ns. This current decreases slowly with increasing regeneration time T due to the erosion of the soot layer. The time lag between application of the voltage and distributed spark breakdown in the filter can vary between few hundred nanoseconds and tens of microseconds. The much shorter time required to establish resistive current flow may be explained by the much smaller size of the microgaps that require breakdown, i.e. the voltage across each small gap will be far above its individual breakdown voltage facilitating very fast breakdown and current flow [14].

If the resistive current is low, and a sufficiently high voltage is retained for ~ 1 μs, a spark may form in the filter, Fig. 3, 6a and 6b. In contrast to the DC high voltage
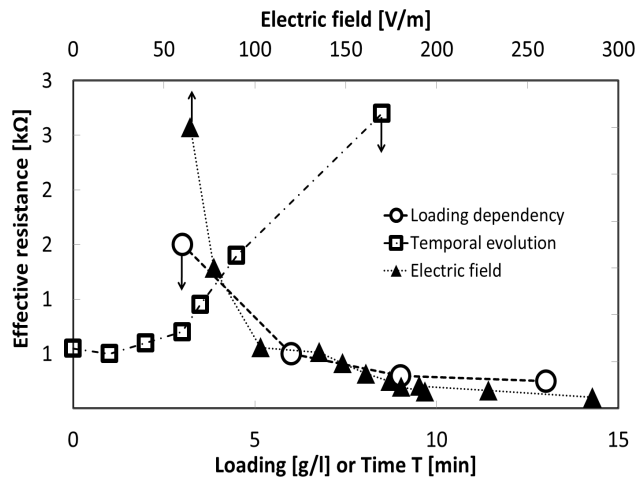
Figure 7: The initial voltage decay due to resistive current flow before spark formation can be considered a simple capacitor discharging though a constant resistance. The voltage measured across the capacitor is then simply given as $V(t) = V_0\, e^{\frac{-t}{RC}}$ where V_0 is the breakdown voltage, R is the effective filter resistance and C is the energy storage capacitance. The effective resistance of the filter increases throughout regeneration as soot is removed $\square$. Note that this particular regeneration was run slowly (breakdown frequency 16 Hz) to collect waveforms, this influence the regeneration time T. The effective filter resistance is also influenced by the electric field (V_0/central HV-Gnd electrode distance) applied at breakdown $\blacktriangle$ and the filter soot loading $\bigcirc$.

breakdown in the spark gap the breakdown in the filter can be considered an impulse breakdown. The voltage has to remain at values above breakdown voltage for a sufficient length of time to facilitate breakdown within the statistical and formative limits [14]. In case of an empty filter leakage currents flow into stray capacitances only, voltage dissipation is slow and the probability for spark formation at or above gap breakdown voltage is high. If, however, a sooty resistive path to ground is present at breakdown voltage, spark formation is initially prevented as the capacitor is depleted too fast. Slow erosion during the microdischarge stage eventually enables spark breakdown after regeneration time T. A larger capacitor >700 pF can facilitate spark breakdown more quickly but will incur raised energy demands.

As a first approximation, the processes in the filter at the very beginning of regenerating a freshly loaded filter and for the first 300 - 500 ns after breakdown can be considered being similar to a capacitor discharging via a simple ohmic resistor, and hence an effective filter resistance can be evaluated if the resistance of the spark gap is assumed to be zero. Examples of effective filter resistances calculated from experimental data are shown in Fig. 7 and are in the order of few hundred to thousands of Ω. Due to the structure of the filter substrate and the soot layer, breakdown occurs distributed over a larger volume in the filter rather than a single spark current channel and the effective resistance of the whole filter decreases dramatically compared to pre-breakdown. Below
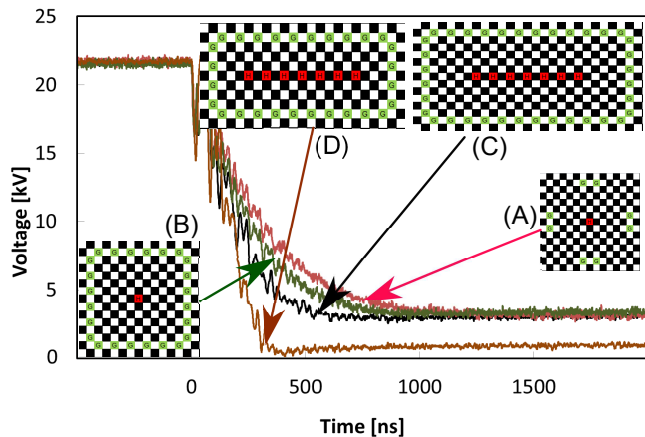
Figure 8: The geometric distribution of grounds and HV electrodes at constant voltage influences the initial resistive current flow.

breakdown voltage few highly resistive conductive paths are available through the soot layer and the electrical resistivity is governed by percolation theory [15], and no direct paths are present between the electrodes themselves as the high voltage electrodes are located in a clean filter channel. At high voltage, however, a number of continuous, parallel current paths to ground are established due to localized breakdown processes.

The effect of electrode geometry on the initial breakdown is a direct consequence of the distribution of the resistive current in the filter volume. The larger the number of grounded electrodes available to the high voltage electrodes, the larger the current and the faster the capacitor charge is depleted, Fig. 8 A, B, C.

Due to soot removal the effective resistance increases steadily during regeneration, Fig.7. Furthermore, the effective resistance decreases as the amount of deposited soot increases. The electric field present between the high voltage and grounded electrodes at breakdown also influences the effective resistance. For these measurements the voltage was increased for one electrode geometry. Changing the distance between the HV and grounded electrodes has a similar effect, which can be seen by comparing (C) and (D) in Fig. 8. Interestingly, in both cases the microdischarge erosion of the soot is not accelerated despite the larger current flow. Indeed, the most effective regeneration voltage applied at breakdown is quite narrowly defined for a given electrode arrangement and also depends somewhat on the regeneration stage. Too low a voltage prevents sufficient breakdown and current flow in the filter to expedite slow erosion, too high a voltage, and spark formation is hindered as the capacitor is depleted too quickly. The semi-automatic regeneration system varies the voltage between ~ 18 and 25 kV for the typical electrode geometries used, allowing control of regeneration modes.

During the microdischarge stage some charge may be retained in the capacitor, Fig. 3. The residual voltage can be measured across the capacitor (V_1) and across the filter (position 2), indicating that the spark gap remains conducting longer than the filter. This may be due to the distribution of current in a larger volume in the latter, as the current flowing through the individual microscale gaps falls below a critical level, their

(a) Removal uniformity
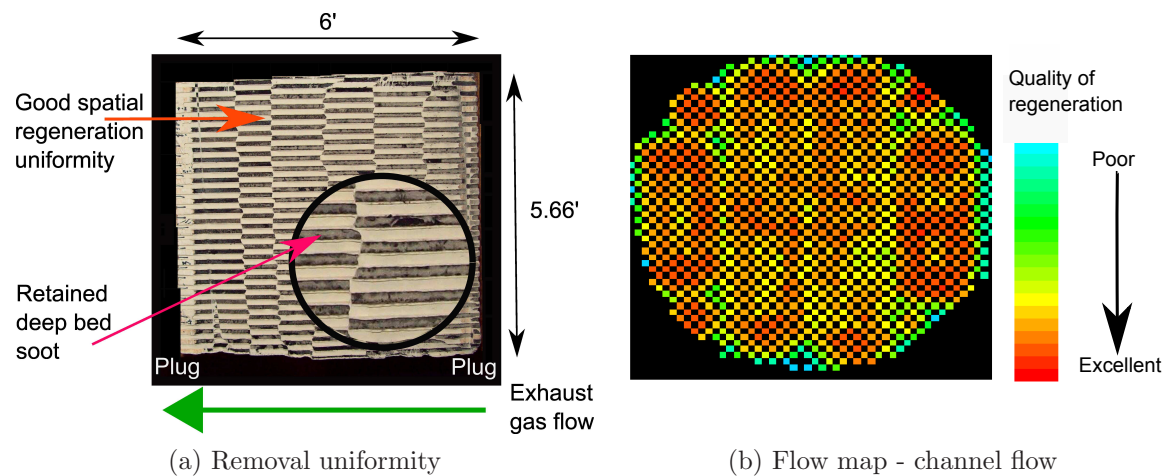
(b) Flow map - channel flow

Figure 9: (a) A sectioned, regenerated filter shows good regeneration uniformity along an individual channel and among the channels in the filter volume. Deep bed soot is retained, but the cake layer is removed.(b) Pressure-drop mapping of a regenerated filter. The flow varies marginally within the regenerated areas, indicating good uniformity and regeneration quality. Low flow is observed in non-regenerated areas (filter rim, channels containing grounded electrodes, channels in-between high voltage electrodes.)

individual resistance quickly increases to open circuit. In all cases the initial effective filter resistance is a good indicator of the overall regeneration duration to clear all accumulated soot.

4. Long term operation

In order to assess the long term behaviour of the pulsed discharge regeneration system a filter was repeatedly loaded and regenerated. The excellent regeneration uniformity along the channel and in the filter volume is shown in the filter section in Fig. 9a. Almost all of the cake layer is removed, but soot remains in the filter walls. A flow map [3], which allows for a qualitative comparisons of the channel flow rates and therefore levels of regeneration is shown in Fig. 9b. During loading the pressure drop over the filter was monitored. A typical sawtooth pressure curve for a single loading is shown in Fig. 10a (insert). The initial fast rise in pressure is due to deep bed soot deposition and a rapid rise in filter temperature from ambient to $\sim 400°$C. The rise then slows and enters a quasi-linear stage over the remaining loading cycle, where soot is mainly deposited as a cake layer. The risetime of the differential pressure is a good measure of regeneration efficiency, after correction for variations in ambient temperature. The time for each consecutive filter loading to reach the maximum engine back pressure of 235 mbar is shown in Fig. 10b. Eighteen loading and regeneration cycles were conducted in total. After a conditioning period of ~ 7 loadings steady state operation is reached where all deposited soot is removed by the regeneration system. The total soot mass deposited and removed from the filter after 18 cycles was ~ 100 g, each discharge pulse on average

(a) Retained deep bed soot
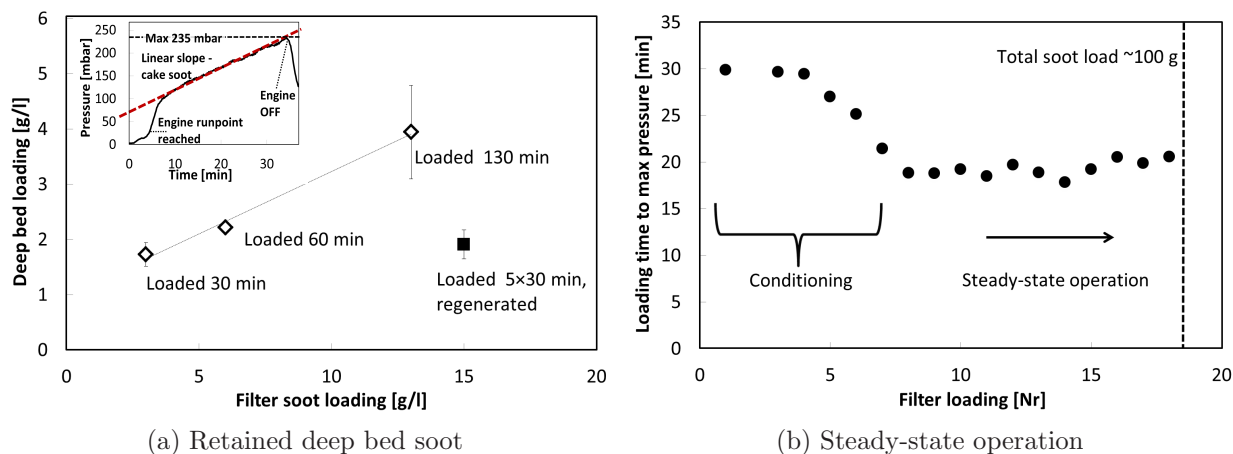

(b) Steady-state operation

Figure 10: (a) (insert) A typical on-engine loading curve for a filter already regenerated several times. With increasing soot loading the differential pressure over the filter increases. (a) Deep bed soot loading increased with overall soot loading for a singly loaded filter. During regeneration some but not all of the deep bed soot is removed.(b) The loading time to reach a given maximum back pressure reduced during the conditioning period and then reaches a steady-state value. The total soot loaded and removed from the filter (volume restriced to V=3l) was ≈ 100 g.

removing a few mg of soot.

Comparing the weight of filter samples after regeneration and heat treatment, where all the soot is removed, showed that the deep bed soot mass increases steadily with total soot loading, as shown in Fig. 10a. Furthermore, it has been observed that the soot retained after regeneration first increases during conditioning until reaching a steady-state value of $\sim$ 2g/l. Loading and regenerating a filter several times keeps the deep bed soot mass lower than in a non-regenerated filter loaded once for the same total time span. This indicates that part of the deep bed soot is removed by the discharge and part remains in the filter walls. The initial conditioning period, Fig. 10b, where the time to bring the filter to the same soot loading slowly decreases, was found to be mainly due to a stepwise increase in deep bed loading up to the steady-state value.

5. Conclusions

Removal of diesel particulate matter from DPFs by pulsed discharges has been investigated with emphasis on the regeneration process. Application of a high voltage pulse to a freshly loaded filter leads to the formation of microdischarges along the filter channels. The magnitude of the initial effective filter resistance is influenced by the electrode geometry, the voltage applied at breakdown and the soot loading, and increases during regeneration as soot is removed. It has been observed that the duration of the first, microdischarge stage of regeneration is increased for a higher initial resistive current/lower effective filter resistance. This is due to the statistical nature of impulse

breakdown, where a sufficiently high voltage has to be retained over the filter for a length of time for a spark to form. By combining rectangular electrode geometry, optimized voltage and energy storage capacitor size the regeneration can be accelerated.

Long term testing of regeneration proved it to be robust, non-destructive and potentially low cost. Furthermore, the technique delivers good spatial and temporal results and does not produce ash. Regeneration behaviour is not affected by soot aging, accumulation of moisture or cell size (100, 200, 300 cpsi). Filters with loadings between 3 g/l and 16 g/l have been regenerated successfully, which removes the need to closely monitor the soot loading in the filter as is the case with oxidative methods. As the pulsed discharge removes virtually the entire cake layer but retains deep bed soot in the channel walls, the filter is expected to maintain a very high particulate matter filtration efficiency throughout operation. This is in contrast to oxidative methods where filtration efficiency has to be re-established after regeneration.

Acknowledgments

[1] C. Buzea, I. I. P. Blandino, and K. Robbie. Regeneration of diesel particulate filters using atmospheric plasmas. *Biointerphases*, 2:MR17–MR172, 2007.

[2] J. Yang, M. Stewart, G. Maupin, D. Herling, and A. Zelenyuk. Single wall diesel particulate filter (DPF) filtration efficiency studies using laboratory generated particles. *Chemical Engineering Science*, 64(8):1625 – 1634, 2009.

[3] A. M. Williams, C. P. Garner, J.E. Harry, Hoare D.W., D. Mariotti, K.S. Ladha, J.W. Proctor, Y. Yang, and J.G.P Binner. Low power auto selective regeneration of monolithic wall flow diesel particulate filters. *SAE Technical Paper*, pages 2009–01–1927, 2009.

[4] M. Okubo, T. Kuroki, S. Kawasaki, K. Yoshida, and T. Yamamoto. Continuous regeneration of ceramic particulate filter in stationary diesel engine by nonthermal-plasma-induced ozone injection. *Industry Applications, IEEE Transactions on*, 45(5):1568 –1574, 2009.

[5] M. Okubo, T. Miyashita, T. Kuroki, S. Miwa, and T. Yamamoto. Regeneration of diesel particulate filter using nonthermal plasma without catalyst. In *Conference Record of the Industry Applications Conference, 2002. 37th IAS Annual Meeting.*, volume 3, pages 1833 – 1840 vol.3, 2002.

[6] S. Yao, C. Fushimi, K. Madokoro, and K. Yamada. Uneven dielectric barrier discharge reactors for diesel particulate matter removal. *Plasma Chemistry and Plasma Processing*, 26:481–493, 2006.

[7] N. Zouzou, C. Agbangla, E. Moreau, and G. Touchard. Diesel particle treatment using a surface dielectric barrier discharge. *Plasma Science, IEEE Transactions on*, 36(4):1354 –1355, aug. 2008.

[8] K. Hensel, S. Sato, and A. Mizuno. Sliding discharge inside glass capillaries. *Plasma Science, IEEE Transactions on*, 36(4):1282 –1283, 2008.

[9] K. Hensel. Microdischarges in ceramic foams and honeycombs. *Eur. Phys. J. D*, 54:141–148, 2009.

[10] S. Sato, K. Hensel, H. Hayashi, K. Takashima, and A. Mizuno. Honeycomb discharge for diesel exhaust cleaning. *Journal of Electrostatics*, 67(23):77 – 83, 2009. 11th International Conference on Electrostatics.

[11] N. Blin-Simiand, P. Tardiveau, A. Risacher, F. Jorand, and S. Pasquiers. Removal of 2-heptanone

by dielectric barrier discharges - the effect of a catalyst support. *Plasma Processes and Polymers*, 2(3):256–262, 2005.

[12] K. Graupner, C.P. Garner, and A.M. Williams. Non-triggered fixed geometry variable voltage spark gap. *In preparation*, 2012.

[13] S. Hashimoto, Y. Miyairi, T. Hamanaka, R. Matsubara, T. Harada, and S. Miwa. Sic and cordierite diesel particulate filters designed for low pressure drop and catalyzed, uncatalyzed systems. *SAE Technical Paper*, pages 2002–01–0322, 2002.

[14] E. Kuffel, W.S. Zaengl, and J. Kuffel. *High voltage engineering fundamentals*, pages 360–365. Butterworth-Heineman, second edition, 2000.

[15] D. Lutic, J. Pagels, and R. Bjorklund. Detection of Soot Using a Resistivity Sensor Device Employing Thermophoretic Particle Deposition. *Journal of Sensors*, 2010:ArticleID 421072, 2010.